



Molecular mechanism of photolysis and photooxidation of poly(neopentyl isophthalate)

Przemyslaw Malanowski^{a,c}, Saskia Huijser^b, Francesca Scaltrò^{a,c}, Rolf A.T.M. van Benthem^{a,*}, Leendert G.J. van der Ven^a, Jozua Laven^a, Gijsbertus de With^a

^aLaboratory of Materials and Interface Chemistry, Eindhoven University of Technology, P.O. Box 513, 5600 Eindhoven, The Netherlands

^bLaboratory of Polymer Chemistry, Eindhoven University of Technology, P.O. Box 513, 5600MB Eindhoven, The Netherlands

^cDutch Polymer Institute (DPI), P.O. Box 902, 5600 AX Eindhoven, The Netherlands

ARTICLE INFO

Article history:

Received 5 August 2008

Received in revised form

8 December 2008

Accepted 3 January 2009

Available online 13 January 2009

Keywords:

Poly(neopentyl isophthalate)

Photolysis

Photooxidation

ABSTRACT

The mechanism of photodegradation of poly(neopentyl isophthalate), an aromatic polyester as model for industrial polyester coatings, was studied on the molecular level. Changes in the chemical structure of molecules caused by UV irradiation (mercury lamp) were investigated using several analytical techniques. Photodegradation leads both to chain scission and to crosslinking, taking place simultaneously as measured by SEC. Extensive exposure results in appreciable amount of insoluble material (gel). Generation of carbonyl C=O and hydroxyl OH/OOH groups in the polymer structure was monitored with ATR-FTIR. MALDI-ToF MS provided detailed structural information on the degradation products of the polyester. In the initial stage of degradation Norrish photocleavage (type I) takes place. Radicals generated in this reaction (photolysis) can directly abstract hydrogen or can react with oxygen creating primarily acid and hydroxyl end groups (photooxidation). Moreover hydrogen abstraction taking place along the polymer backbone followed by oxidation reactions leads to further fragmentation of the polymer chain. The highly informative data provided by MALDI-ToF MS allowed establishing the pathways of photolysis and photooxidation.

© 2009 Elsevier Ltd. All rights reserved.

1. Introduction

Organic coatings are thin, often pigmented layers of a polymer network applied on a substrate. They are used for protection against corrosion and weathering as well as for decoration purposes. The main part of an organic coating is the polymeric binder which consists of a polymer having reactive groups (resin) and often a crosslinker. Most commonly used resins in coating technology are acrylics, polyesters, alkyds and epoxies.

Many factors simultaneously influence the life time of a coating. The combined action of UV radiation, heat and moisture can cause changes in the chemical structure of polymer networks. Such chemical changes influence the physical properties of coatings and consequently lead to failure (cracking, gloss loss, blistering, etc.) and reduction of life time. UV radiation is one of the most important factors affecting degradation [1,2].

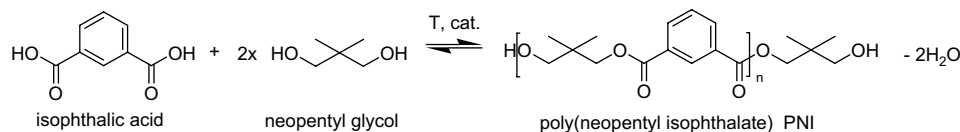
Photodegradation of polyesters like poly(ethylene terephthalate) (PET) and poly(butylene terephthalate) (PBT) has been extensively investigated [3–10]. Day and Wiles studied

photochemical degradation of PET [4–6]. Mainly based on the analysis of volatile products (CO and CO₂) and on FTIR it was suggested that UV absorption by the aromatic ester group induced Norrish (types I and II) photocleavage. Later, Rivaton studied photodegradation of PBT using FTIR supported with chemical derivatization [7,8]. The data obtained confirmed the Norrish (types I and II) photocleavage and resulted in proposing more advanced mechanisms of the photodegradation of the aromatic polyester. However, IR does not provide detailed molecular information. Moreover, some of the products of the photodegradation may not be detected *e.g.* if they have low absorbance, or other absorbances are strongly overlapping. Thus, more detailed characterization of the molecular mechanism of photodegradation is still required.

Among industrially used polyester coatings, those based on neopentyl glycol and phthalic acid isomers, especially isophthalic acid, exhibit the best outdoor durability [11]. Although those polyester coatings are widely used in outdoor application, mainly because of their superior mechanical properties, improvement of their outdoor durability, at least up to the level of *e.g.* acrylic coatings, is still very desirable. This explains the industrial interest in investigations of the mechanisms of degradation in such polyesters, yet only a few papers have been published on this topic up to now [11,12]. Interestingly, in poly(neopentyl isophthalate) (PNI)

* Corresponding author. Tel.: +31 (0)402472029; fax: +31 (0)402445619.

E-mail address: r.a.t.m.v.benthem@tue.nl (R.A.T.M. van Benthem).



Reaction 1. Polycondensation reaction of neopentyl glycol and isophthalic acid.

only Norrish type I photocleavage is possible due to the absence of β -H in the neopentyl glycol moiety, making this polymer very suitable for a model study on a molecular level.

Investigation of the degradation of organic coatings is a complicated process. In most cases chemical changes taking place during UV exposure are studied using overall spectroscopic techniques such as FTIR and UV [11,12]. Since organic coatings consist of polymer networks, the application of molecular analytical techniques such as chromatography and mass spectrometry has been limited. Here, we report on the photolysis and photooxidation of non-crosslinked poly(neopentyl isophthalate) PNI coatings. The mechanism of degradation is investigated using several analytical techniques: ATR-FTIR, SEC and MALDI-ToF MS. The most valuable information with respect to the mechanism of degradation is provided by MALDI-ToF MS. This technique allows studying individual polymer chains as a function of exposure time. In recent years the successful application of this technique to study the mechanisms of thermal and photodegradation of polymers has been demonstrated [13–15], including PBT [16]. The main goal of this work is to present the application of MALDI-ToF MS to study the photodegradation of poly(neopentyl isophthalate) (PNI). In addition, the interpretation of complicated (isotope overlapping) MALDI-ToF MS data was made possible by in-house-developed software for the isotope distribution calculation, resulting in detailed structural information on the products of the photodegradation. Based on these highly informative MALDI-ToF MS data as well as on supportive FTIR and SEC data, the mechanisms of photolysis and photooxidation are proposed.

This paper reports on the mechanism of photolysis and photooxidation of PNI exposed to short wavelength UV radiation ($\lambda \geq 254$ nm) as provided by an Hg lamp. The choice for this spectral range could be questioned from the relevance of such experiments for the outdoor degradation of coatings as the spectrum of the sunlight at the surface of the earth is limited to wavelengths of ≥ 300 nm. However, the main reason for using short wavelength UV radiation concerns the initiation step of photodegradation. It is known that polyesters based on terephthalate have absorbance especially at wavelengths below 310 nm. Thus between 300 and 310 nm an appreciable amount of light is absorbed that can cause photodegradation. In this case Norrish type I photocleavage has been postulated to be the initiation step. On the other hand, polyesters based on isophthalate, like PNI, have absorbance especially below 295 nm. In that case absorption of natural sunlight will be very small and photodegradation will be very slow. This may explain their excellent weathering stability. In this case Norrish type I photocleavage may not be the dominant initiation step and other mechanisms could be involved e.g. due to impurities or imperfect chains. Exposure of PNI to short wavelength UV ($\lambda \geq 254$ nm) ensures that the main photodegradation is due to the intrinsic properties of the material itself. This paper reports on such tests and analyses. In a subsequent paper degradation due to exposure to natural sunlight and similar laboratory tests will be analyzed and compared to the results in the current paper.

This paper investigates the molecular mechanisms leading to fragmentation of the polymer. The mechanism of photocrosslinking, which is the other process simultaneously taking

place during the photodegradation, is not discussed in this work and will be published elsewhere.

2. Experimental

2.1. Materials

The model polyester poly(neopentyl isophthalate) (PNI) used in this study was provided by DSM. This polyester was prepared from isophthalic acid and neopentyl glycol in a bulk polycondensation process (Reaction 1). Titanium(IV) *n*-butoxide ($\text{Ti}(\text{O}i\text{Bu})_4$) was used as the catalyst. The synthesis was performed with an excess of neopentyl glycol resulting in a hydroxyl functional polymer (hydroxyl value 16 mg of KOH/g and acid value 1 mg of KOH/g). M_n values based on titration data and on SEC are equal to 6600 g/mol and 9600 g/mol respectively. Its glass transition temperature T_g , as measured by DSC, was 58 °C. The UV absorption spectrum of PNI is presented in Fig. 1.

2.2. Coating preparation

PNI was dissolved in *N*-methyl-2-pyrrolidone (NMP) (30 w/w%). The solution was applied on an aluminium plate (cleaned with ethanol and acetone) using a doctor blade. Coatings were dried in an oven at 120 °C for 1 h; all NMP was evaporated (checked with FTIR, 1675 cm^{-1}). The thickness of the resulting dry coating was approximately 12 μm .

2.3. UV exposure

The samples were aged using a UVACUBE apparatus equipped with a high pressure mercury lamp (Dr. Hönle AG) emitting radiation in the 254–600 nm range. The spectral power distribution of mercury lamp is shown in Fig. 1. The intensity of the light was measured using a UV Power Puck (EIT Inc.) in the ranges of UVA (400 W/m^2) and UVB (150 W/m^2). The UVACUBE was additionally equipped with a thermostatic aluminium box (68 °C) covered by a quartz glass in which the PNI coatings were placed. Through the thick bottom of the box a thermostatic liquid was purged that was

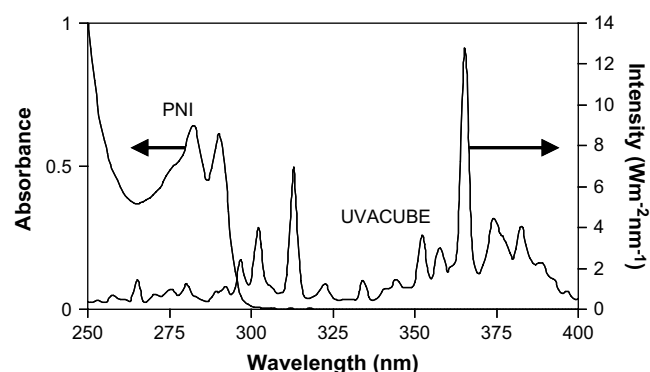


Fig. 1. UV absorption of PNI and spectral power distribution of the light emitted by the mercury lamp in the UVACUBE.

set at 68 °C. All experiments were performed in dry air atmosphere. Exception to this rule is one experiment performed in dry nitrogen atmosphere (Fig. 6). The distance from samples to the lamp was 20 cm. Samples (5 cm × 5 cm) were exposed to UV light for either 10 or 20 h.

2.4. Analytical methods

Attenuated Total Reflectance Fourier Transform Infrared Spectroscopy (ATR-FTIR) was performed using a BioRad Excalibur FTS3000MX spectrometer equipped with a diamond crystal (Golden Gate). Spectra of the surface of the PNI coatings were recorded in the range of 4000–650 cm^{-1} with a resolution of 4 cm^{-1} . For ATR-FTIR spectroscopy a small piece was cut from the coated panel and pressed on the ATR crystal.

Size exclusion chromatography (SEC) was carried out using a WATERS 2695 separation module and a Model 2414 refractive index detector at 40 °C. The injection volume used was 50 μl . The column set consisted of a Polymer Laboratories PLgel guard column (5 μm particles, 50 × 7.5 mm), followed by two PLgel mixed-C columns (5 μm particles, 300 × 7.5 mm). The columns were calibrated at 40 °C using polystyrene standards (Polymer Laboratories, $M = 580$ up to $M = 7.1 \times 10^6$ g/mol). Tetrahydrofuran (Biosolve, stabilised with BHT) was used as the eluent at a flow rate of 1.0 ml/min. Prior to the SEC analysis, the polyester was removed from the substrate and dissolved in THF. In the case of aged polyester the insoluble (crosslinked gel) part of the polymer was removed by filtration (0.2 μm PTFE filter) and the soluble part (concentration ~5 mg/ml in THF) was analyzed. Data acquisition and processing were performed using WATERS Empower 2 software.

Matrix assisted laser desorption ionization time of flight mass spectra (MALDI-ToF MS) were recorded in reflector mode using a Voyager-DE STR instrument. Trans-2-[3-(4-*tert*-butylphenyl)-2-methyl-2-propenylidene] malononitrile was used as a matrix. Samples were prepared by mixing matrix, potassium trifluoroacetate and polymer sample in a volume ratio 4:1:4, with THF as the solvent. Prior to the MALDI-ToF MS test, polyester was removed from the substrate and dissolved in THF. In the case of the aged polyester the insoluble (crosslinked gel) part of the degradation was removed by filtration. The soluble part was analyzed. The Copol Analysis Program by B.B.P. Staal was used to calculate isotopic distributions [17].

Differential Scanning Calorimetry (DSC) was performed using a Perkin-Elmer Pyris 1 calorimeter. The glass transition temperature (T_g) was obtained from the second heating run as the mid-point of the heat capacity transition. The heating rate was 20 °C/min.

Gel fractions were determined gravimetrically. The adhesion of the polyester coating to the aluminium substrate was very high and peeling off the coating for gel fraction measurement was not possible. Instead the weight of the coating together with the substrate was measured first. Then, the polyester was washed off with THF and the weight of the bare substrate was measured. The soluble part of polyester was separated from the gel by filtration (0.2 μm PTFE filter). After evaporation of THF (24 h at 75 °C, vacuum oven) the weight of the soluble fraction was measured. Knowing the weights of the coating with the substrate, the bare substrate and the soluble fraction, the weight of the gel fraction was calculated.

UV spectroscopy was performed using a UV/VIS/NIR spectrometer Lambda 900 (Perkin-Elmer). Spectra were collected in the range of 500–200 nm. For such a measurement PNI was dissolved in chloroform and placed in quartz cuvettes. The concentration of PNI in chloroform was 0.177 g/dm³.

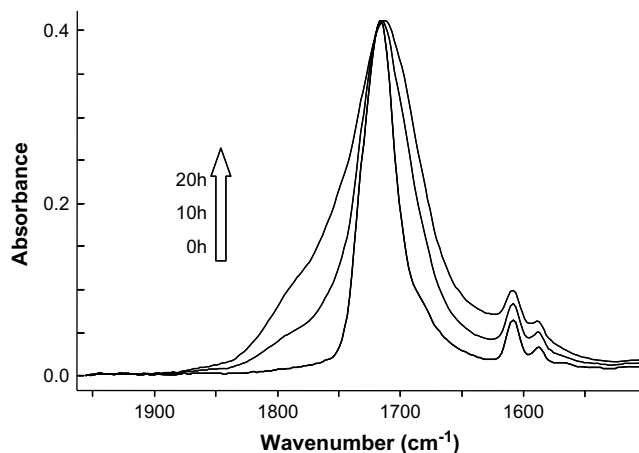


Fig. 2. ATR-FTIR spectra (region of C=O band) of the polyester coating surface after UV irradiation for 0, 10 and 20 h.

The spectral power distributions of light emitted by the mercury lamp in the UVACUBE was measured using an AVS SD2000 Fiber Optic Spectrometer (Avantes).

3. Results and discussion

3.1. ATR-FTIR analysis

ATR-FTIR spectroscopy was used to monitor the formation and disappearance of functional groups at the polymer surface during photodegradation. Spectra of the polyester irradiated in air atmosphere (Figs. 2 and 3) exhibit significant changes in the carbonyl region (1850–1600 cm^{-1}) and in the hydroxyl/hydroperoxide region (3600–2500 cm^{-1}). The changes in the carbonyl region are probably caused by the following groups formed during degradation: anhydride (stronger band at 1780–1770 cm^{-1} ; weaker band at 1725–1715 cm^{-1}); carboxylic acids: aliphatic (1725–1700 cm^{-1}) and aromatic (1700–1680 cm^{-1}); aldehydes: aliphatic (1730–1725 cm^{-1}) and aromatic (1710–1690 cm^{-1}) [18]. Whereas a sharp absorption in the hydroxyl region (3600–3300 cm^{-1}) is generally believed to be characteristic for non-hydrogen bonded hydroxyl groups, in our case (Fig. 3) a broad absorption is observed, indicating hydrogen bonded hydroxyl and carboxyl groups. Hydrogen bonded, carboxylic hydroxyl groups are known to give a broad absorption band between 2500 and 3600 cm^{-1} (Fig. 3).

PNI contains two ester carbonyl groups in each repeating unit. These groups may well serve as hydrogen bond acceptors for different types of hydroxyls formed during the degradation. Other carbonyl groups, originating from degradation, may have a similar role.

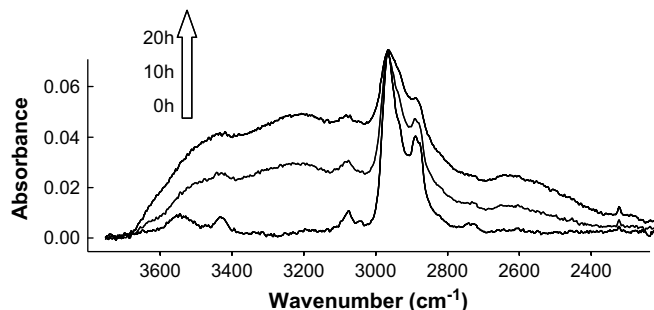


Fig. 3. ATR-FTIR spectra (region of OH and OOH band) of the polyester coating surface after UV irradiation for 0, 10 and 20 h.

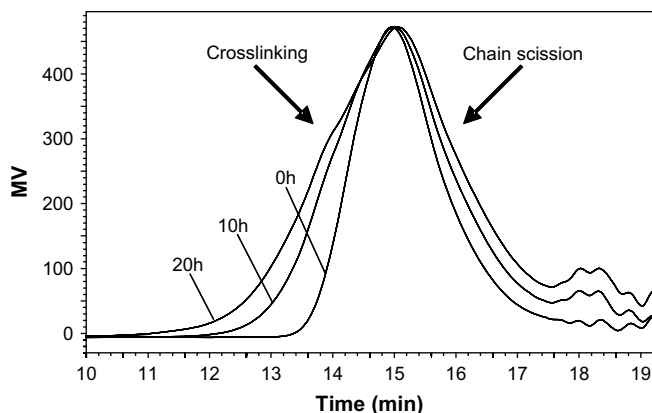


Fig. 4. SEC chromatograms of polyester UV irradiated for 0, 10 and 20 h.

3.2. SEC analysis

Size Exclusion Chromatography was performed to determine changes in molecular weight. Fig. 4 shows SEC chromatograms of the polyester aged for 0, 10 and 20 h. As can be seen, molecules both with higher and lower molecular weight are formed during UV exposure. Photodegradation leads to break down of the polymer chains resulting in a decreased number average molecular weight (M_n) as presented in Table 1. Simultaneously some of the radicals formed during this process may recombine and form crosslinked molecules leading to the increase of weight average molecular weight (M_w), Table 1. During this process a high molecular weight sol fraction (crosslinked molecules, still soluble) is formed first. Extensive crosslinking leads to gel (insoluble crosslinked molecules) formation. The insoluble part – gel – was removed by filtration and its content was calculated as explained in Section 2. The gel fraction reached 17% after 10 h and 23% after 20 h of UV exposure.

3.3. MALDI-ToF MS analysis

In this experiment the soluble degradation products were identified using MALDI-ToF MS. All polymer molecules discussed consist of the same repeating unit (molecular mass of the isophthalic acid and neopentyl glycol, H_2O subtracted, 234 g/mol). Polymer chains are terminated with various end groups. Exceptions to this general description are cyclic oligomers (no end group) and anhydride or hemiacetal groups being present in the polymer chains. All identified oligomers are described and listed in Table 2 including the mass charge ratio (m/z) of the most abundant peak of that oligomer. Fig. 5 shows enlarged parts of the MALDI-ToF MS spectra (one repeating unit) of the polyester, non-aged (A), aged for 1 h (B), 10 h (C) and 20 h (D), respectively. The main structure of the non-aged polymer (Fig. 5A) is a sequence of repeating units terminated with neopentyl alcohol (Structure 1a, Table 2). Additionally, structures 1b, 6, 8a and 8b were identified. These are thought to be species inherent to polycondensation reactions (cyclic oligomers: 8b) or species being formed during

Table 1
Changes in M_n , M_w and PDI of PNI aged for 0 h, 10 h and 20 h, as obtained by SEC.

	M_n [g/mol]	M_w [g/mol]	PDI
0 h	9650	17 300	1.8
10 h	9550	24 500	2.5
20 h	9400	32 700	3.5

polycondensation as a result of thermal- or thermo-oxidative degradation reactions. Already 1 h of UV exposure (Fig. 5B) results in the formation of new structures. Ageing for 10 and 20 h (Fig. 5C and D) leads to an increase of existing structures and to the formation of many new products as photodegradation proceeds. Fig. 6 shows enlarged parts of MALDI-ToF MS spectra (one repeating unit) of the PNI aged for 1 h in air (6A) and 1 h in nitrogen (6B).

The mass of a molecule shows up in MALDI spectrum as a distribution of masses (“isotopic distribution”) around a mean value, due to the occurrence of isotopes of C, O, N, etc. The shape of the isotopic distribution is an indication of the atomic composition of the structure. There are two main problems when analyzing isotopic distributions originating from two structures that have (almost) similar masses. First of all, molar masses of two molecules that differ by less than the resolution of the equipment (typically ~ 0.5 Da) will show up as a single peak and distinguishing them is impossible. This phenomenon is usually referred to as “isotope interference” [17]. Secondly, when two structures have mean values that differ by ~ 4 Da or less, these isotopic distributions overlap into a cluster of isotopic distributions (“isotope overlap” [17]). For example the isotopic distribution described by number 2 (Figs. 5 and 7) is a result of isotopic distributions originating from two macromolecular species (2a, 2471 m/z and 2b, 2469 m/z , Table 2). This phenomenon complicates the interpretation of the data. In order to overcome the problem of isotope overlap and to identify the products of degradation, in-house-developed software was used [17]. This program calculates the isotopic distributions for given (expected) chemical structures and compares them to the experimental data. The usefulness of this software has been already proven in the investigation of the chemical composition and the topology of poly(lactide-co-glycolide) [19]. In our experiment ultimately 15 isotopic distributions were found representing 28 molecules. The same isotopic distributions were found in different repeating units from 1000 m/z up to 7000 m/z . Fig. 7A shows an experimental and a simulated enlarged part (one repeating unit) of the MALDI-ToF MS spectrum of PNI aged for 20 h. In order to better visualize the experimental and simulated isotopic distributions, Fig. 7A was split into A1 and A2. In all cases a good match between experimental and simulated data was found, which confirms the presence of the molecules listed in Table 2.

One of the disadvantages of MALDI-ToF MS is mass discrimination, i.e. smaller molecules have a higher possibility for being detected than molecules of higher molecular weight. For polymers with a higher polydispersity index as in this case (photodegradation leads to chain scission and crosslinking), smaller molecules can be expected to dominate the spectra. This effect could explain why primarily products from photolysis and photooxidation (which mainly lead to chain scission) are observed, and no still soluble products of crosslinking and chain extended species are detected.

4. Mechanism of photolysis and photooxidation

As reported in many papers [3–9], Norrish type I photocleavage is the main initiation step of photodegradation of aromatic polyesters. The ester group can be cleaved at 3 different positions (Scheme 1, cases: A–C), creating 6 different primary radicals (alkoxy A-1, acyl A-2, alkyl B-1, carboxyl B-2, formate C-1, phenyl C-2). Rearrangements, oxidation and termination reactions of these radicals are discussed and illustrated below according to the above mentioned cases (A – Scheme 2, B – Scheme 3, C – Scheme 4). Moreover the hydrogen abstraction in the polymer backbone followed by oxidation reactions is elucidated (Schemes 5 and 6). Combinations of a number and a small letter, e.g. 1a, refer to structures Table 2.

Table 2
Structures of the molecules identified with MALDI-ToF MS.

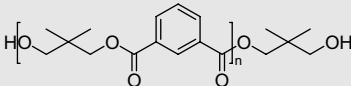
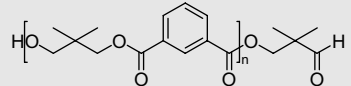
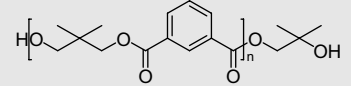
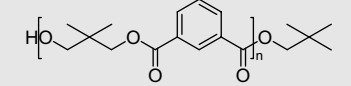
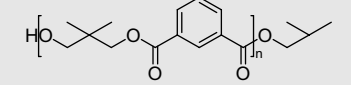
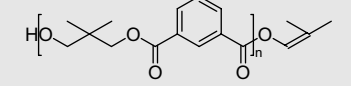
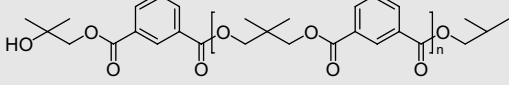
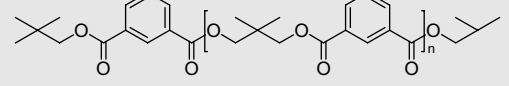
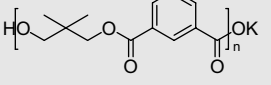
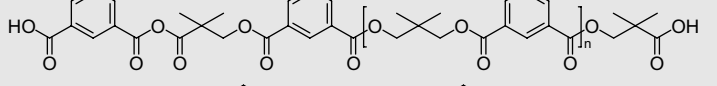
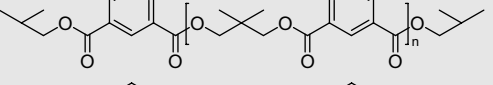
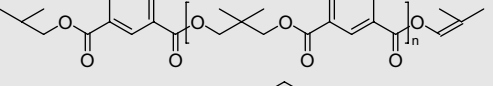
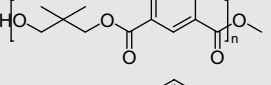
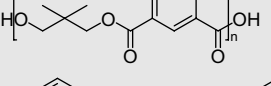
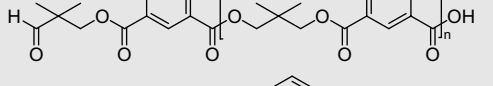
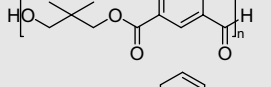
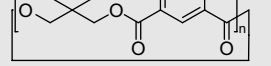
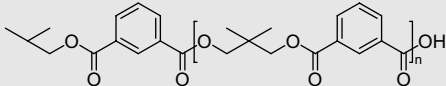
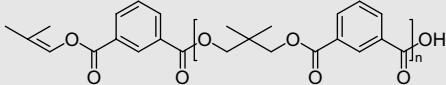
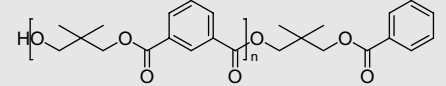
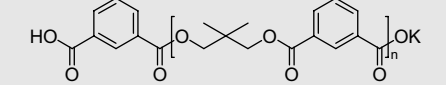
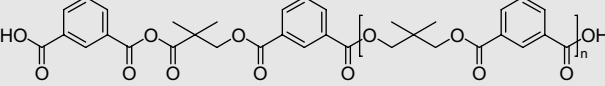
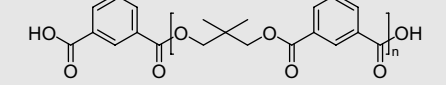
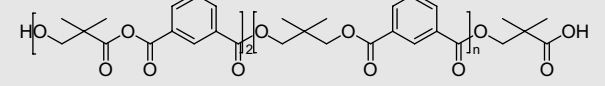
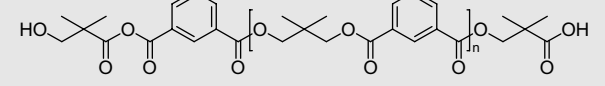
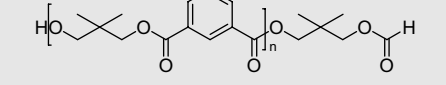
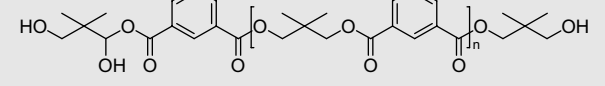
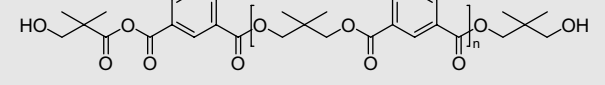
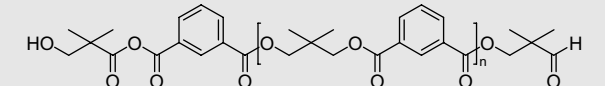
Isotopic distribution number	Structure	<i>n</i>	M ⁺ K ⁺ (most abundant peak)
1	a 	10	2485
	b 	10	2483
2	a 	10	2471
	b 	10	2469
3	a 	10	2455
	b 	10	2453
4	a 	9	2441
	b 	9	2439
5	c 	10	2437
	a 	8	2427
	b 	9	2425
6	c 	9	2423
		10	2413
7	a 	10	2399
	b 	9	2397
8	a 	10	2383
	b 	10	2381

Table 2 (continued)

Isotopic distribution number	Structure	<i>n</i>	M ⁺ K ⁺ (most abundant peak)
9	a 	9	2369
	b 	9	2367
10	a 	9	2355
	b 	9	2351
11		8	2327
12		9	2313
13		7	2293
14	a 	8	2279
	b 	9	2279
15	a 	8	2267
	b 	8	2265
	c 	8	2263

4.1. Norrish type I photocleavage, case A (Scheme 2)

Due to Norrish type I photocleavage of the ester group, in case A (Schemes 1 and 2) an alkoxy radical A-1 ($\cdot\text{O}-\text{CH}_2-$) and an acyl radical A-2 ($-\dot{\text{C}}=\text{O}$) are formed.

4.1.1. Alkoxy radical A-1

The alkoxy radical A-1 can be rearranged by formaldehyde elimination (Scheme 2) to the stable tertiary alkyl radical A-3 ($-\dot{\text{C}}<$). Hydrogen abstraction by this alkyl radical leads to the formation of an isobutyl end group (Structures 3a, 4a, 4b, 5b, 5c and 9a). Alternatively the tertiary alkyl radical A-3 can disproportionate (Scheme 2) to an isobutene end group (Structures 3b, 5c and 9b). The presence of isobutyl and isobutene end groups was indicated by

MALDI already after 1 h of irradiation both in air and in nitrogen conditions (clustered isotopic distribution 3, Figs. 5 and 6), proving that photocleavage according to case A takes place.

Furthermore the tertiary alkyl radical A-3 can also undergo oxidation processes (Scheme 2) resulting in the formation of a tertiary butanol (Structures 2a and 4a). To this end for example, the tertiary alkyl A-3 first reacts with oxygen to form a peroxy radical, which after hydrogen abstraction forms a hydroperoxide. Decomposition of the hydroperoxide followed by hydrogen abstraction leads to the formation of the tertiary butanol end group.

The alkoxy radical A-1 formed due to photocleavage, case A (Schemes 1 and 2), can also abstract hydrogen (Scheme 2) and form a neopentyl glycol end group (Structure 1a). Since this end group is

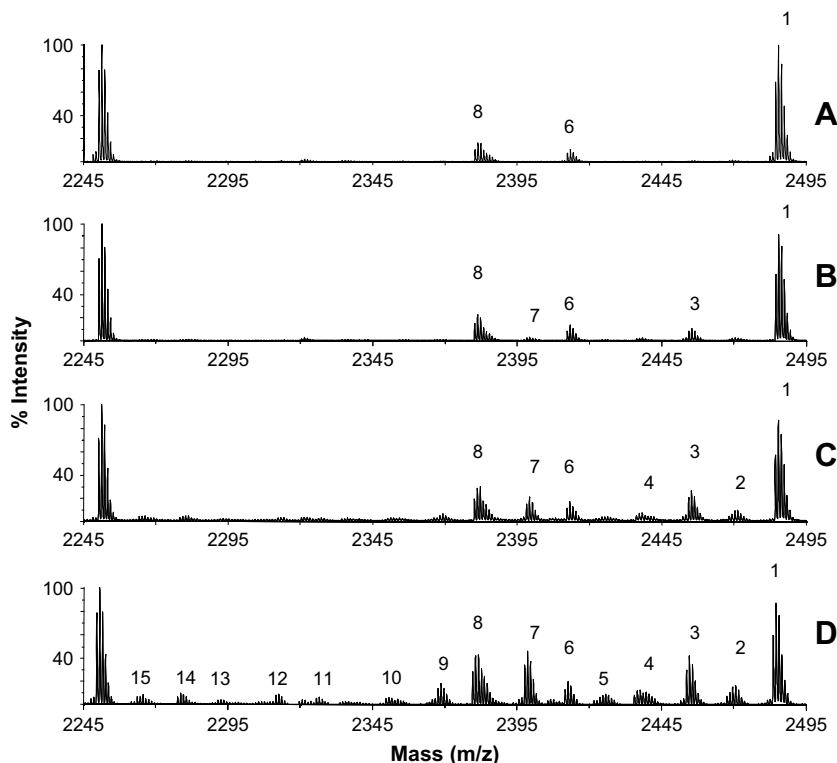


Fig. 5. Enlarged parts of MALDI-ToF MS spectra (one repeating unit) of PNI non-aged (A), aged for 1 h (B), 10 h (C) and 20 h (D). The numbers of the isotopic distributions correspond to the structures listed in Table 2.

also present in the virgin polymer, this does not lead to a new isotopic distribution in the MALDI spectrum. However, the broad band formed in the hydroxyl/hydroperoxide region of the ATR-FTIR spectra (Fig. 3) suggests that such hydroxyl groups are formed.

4.1.2. Acyl radical A-2

The Norrish type I photocleavage of the ester group, case A (Schemes 1 and 2), leads also to an acyl radical A-2 formation. After hydrogen abstraction of this radical a phthalaldehyde end group is formed (Structure 8a). This structure together with a cyclic oligomer (Structure 8b) is represented by the clustered isotopic distribution 8 (Figs. 5 and 7) and was identified already before ageing. Although this isotopic distribution seems to rise in comparison to the isotopic distribution 1 (representing virgin polymer, Fig. 5), it cannot be concluded beyond doubt that more of

these molecules are being formed, because MALDI-ToF MS is not a quantitative technique.

In the presence of oxygen, the acyl radical A-2 can undergo oxidation (Scheme 2) to a phthalic acid end group (Structures 7a, 7b, 9a, 9b, 11 and 12). During this process a peracid is formed first. Decomposition of the peracid leads to a carboxyl radical, which after hydrogen abstraction finally forms the phthalic acid end group. During MALDI ionization of those molecules, the proton of an acid end group $-C(O)OH$ can be replaced with potassium $-C(O)OK$. This phenomenon results in an extra isotopic distribution in the MALDI spectrum (Structures 4c and 10b). Moreover the presence of acids was indicated by ATR-FTIR spectroscopy, in the hydroxyl and carbonyl region (Figs. 2 and 3).

In addition the acyl radical A-2 can undergo decarbonylation and form a benzoic end group (Structure 10a).

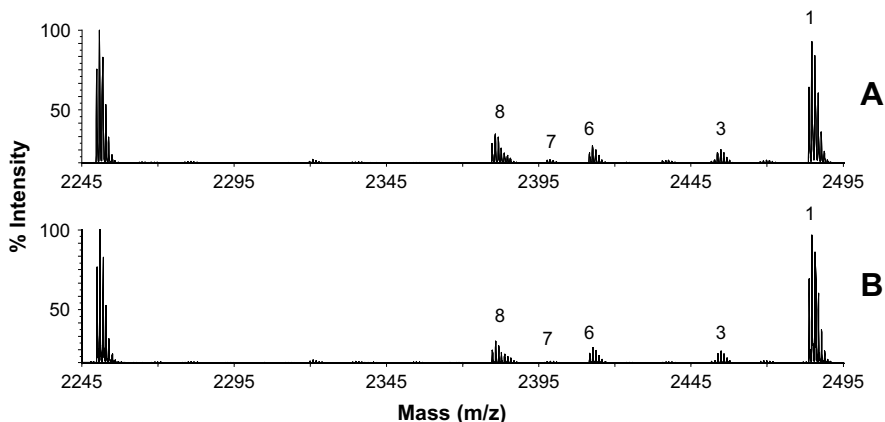


Fig. 6. Enlarged parts of MALDI-ToF MS spectra (one repeating unit) of PNI aged for 1 h in air conditions (A) and aged for 1 h under nitrogen (B). The numbers of the isotopic distributions correspond to the structures listed in Table 2.

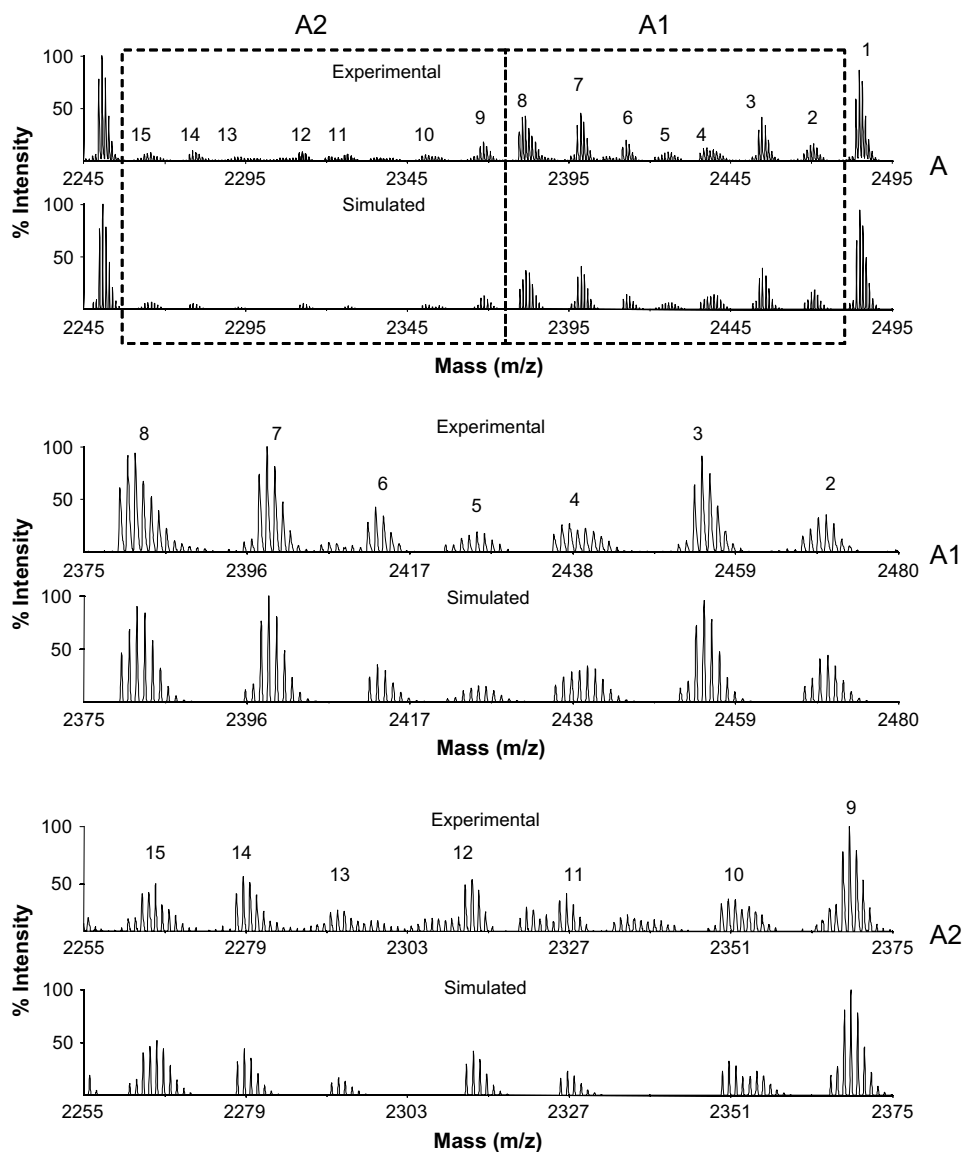
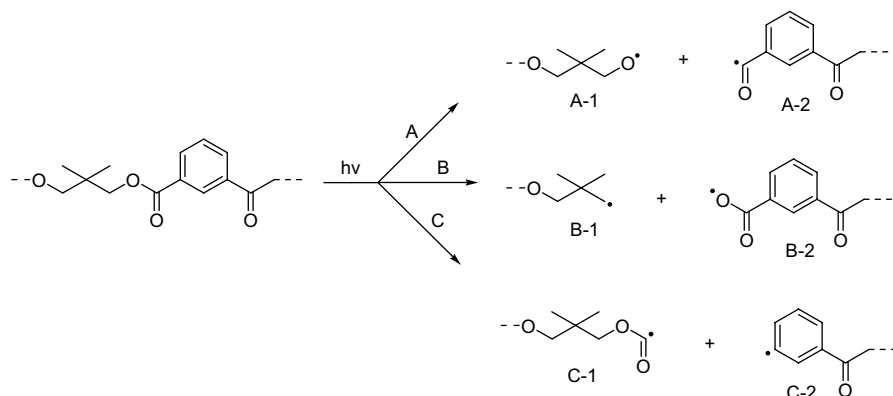
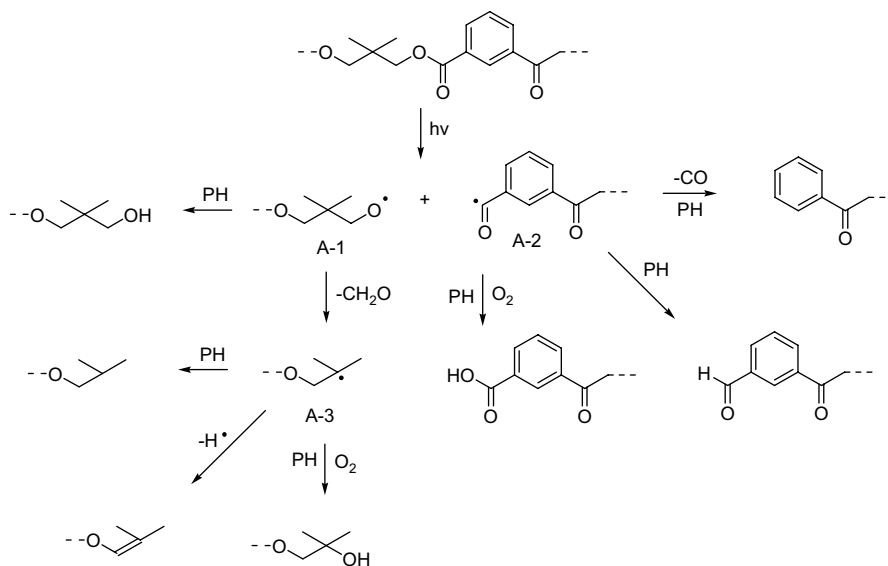


Fig. 7. Experimental and simulated enlargements of the MALDI-ToF MS spectrum of PNI aged for 20 h (A; one repeating unit: 2245–2495 m/z), (A1; enlargement of repeating unit: 2375–2480 m/z), (A2; enlargement of repeating unit: 2255–2375 m/z). The numbers of the isotopic distributions correspond to the structures listed in Table 2. The calculation was performed for 15 isotopic distributions. Between isotopic distributions 10/13 additional small isotopic distributions were found. Those small isotopic distributions presumably are superpositions of other larger ones and for them simulation was not performed.



Scheme 1. Norrish type I photocleavage of ester group, cases: A–C.



Scheme 2. Photolysis and photooxidation pathways resulting from Norrish type I photocleavage A.

4.2. Norrish type I photocleavage, case B (Scheme 3)

As a result of Norrish type I photocleavage of the ester group, case B (Schemes 1 and 3), an *alkyl radical B-1* ($\text{CH}_2\cdot$) and a *carboxyl radical B-2* ($-\text{C}(\text{O})\text{O}\cdot$) are formed.

4.2.1. Alkyl radical B-1

Hydrogen abstraction of an *alkyl radical B-1* (Scheme 3) leads to a neopentyl end group (Structures 2b and 4b). The reaction of an *alkyl radical B-1* with oxygen results in an *alkoxy radical A-1* (also formed as a primary radical), the propagation of which was described above.

4.2.2. Carboxyl radical B-2

The *carboxyl radical B-2* can abstract a hydrogen atom (Scheme 3) and form a phthalic acid end group (Structures 7a, 7b, 9a, 9b, 11 and 12). This end group was already identified after 1 h of ageing both in air and in nitrogen atmosphere (Fig. 6). In the absence of oxygen, a phthalic acid end group can be formed only due to the above mentioned mechanism. Its identification proves the occurrence of photocleavage B.

In addition the *carboxyl radical B-2* can undergo decarboxylation and form a benzoyl end group (Structure 10a).

4.3. Norrish type I photocleavage, case C (Scheme 4)

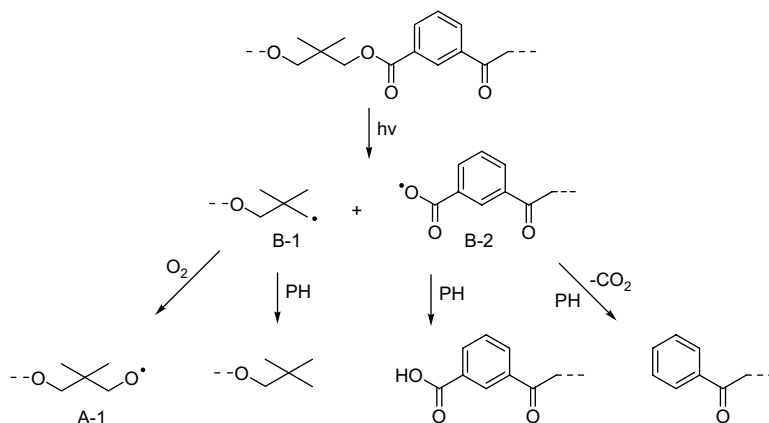
Chain scission due to Norrish type I photocleavage of the ester group, case C (Schemes 1 and 4), results in a *formate radical C-1* ($-\text{O}-\text{C}\cdot=\text{O}$) and the corresponding *phenyl radical C-2* ($\text{C}_6\text{H}_4\cdot$).

4.3.1. Formate radical C-1

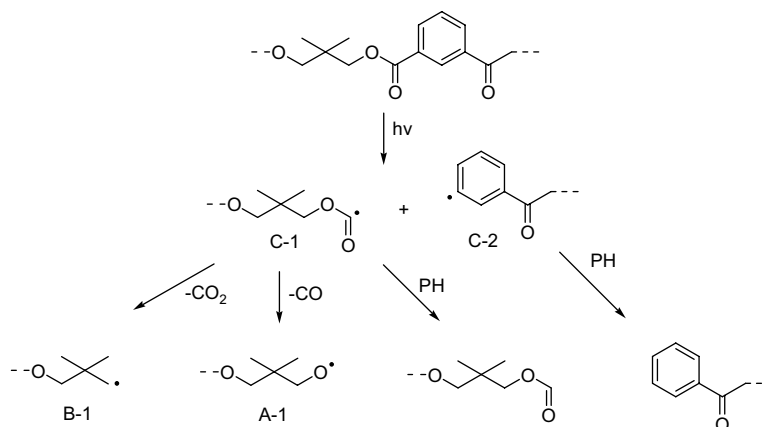
A *formate radical C-1* can undergo decarbonylation or decarboxylation (Scheme 4). The first reaction leads to the formation of CO and an *alkoxy radical A-1*, the second to the formation of CO_2 and an *alkyl radical B-1*. The hydrogen abstraction of a *formate radical C-1* would lead to the formation of a formate end group (Structure 14b). The m/z ratio of 2279 seems to correspond to this structure. However, it can also be attributed to, for example, oligomers terminated with a pivalic acid end group and also containing an anhydride (Structure 14a).

4.3.2. Phenyl radical C-2

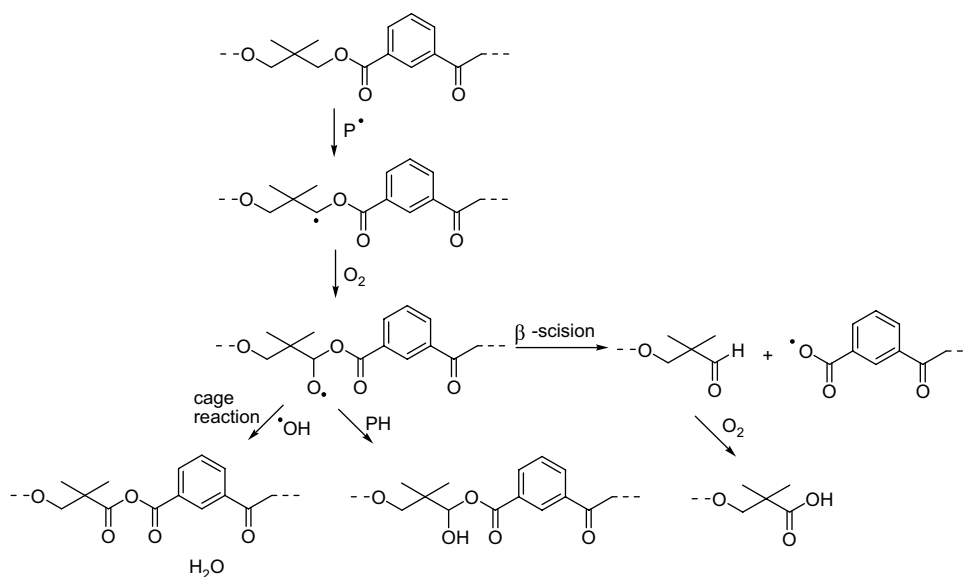
As illustrated in Scheme 1, case C and Scheme 4, the *phenyl radical C-2* can be formed by photocleavage of the ester group. It can be also formed by decarbonylation of the *acyl* (Scheme 2) or by decarboxylation of the *carboxyl radicals* (Scheme 3). *Phenyl radicals C-2* can abstract hydrogen (Schemes 2–4) and form a benzoic end group (Structure 10a).



Scheme 3. Photolysis and photooxidation pathways resulting from Norrish type I photocleavage B.



Scheme 4. Photolysis and photooxidation pathways resulting from Norrish type I photocleavage C.



Scheme 5. The hydrogen abstraction in the polymer backbone followed by oxidation reactions.

Although several of the possible photocleavage C products could be attributed to isotopic distributions observed in the MALDI-ToF MS spectra, these isotopic distributions could also be explained on the basis of photocleavages A and B and/or oxidation reactions from them. Hence there is no direct proof for the occurrence of photocleavage C.

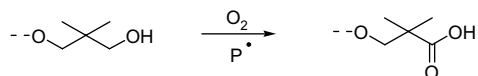
4.4. Hydrogen abstraction in the polymer backbone followed by oxidation reactions (Scheme 5 and 6)

The impact of hydrogen abstraction of all above mentioned processes is considerable. As was shown, polymer free radicals and later formed oxy- and peroxy-radicals can abstract hydrogen. The by far most labile hydrogen atoms on the polyester backbone are located in the α -position of the ester group. *Macromolecular alkyl radicals* (Scheme 5) ($-\text{C}^{\bullet}\text{H}-\text{O}-\text{C}(\text{O})-$) result from hydrogen

abstraction on those positions. Such *macroalkyl radicals* can react with oxygen. First a peroxy radical is formed, which in turn, by hydrogen abstraction creates hydroperoxide. This hydroperoxide can undergo a homolysis reaction and the *macroalkoxy radical* ($-\text{C}(\text{O}^{\bullet})\text{H}-\text{O}-\text{C}(\text{O})-$) is formed (Scheme 5). The above described reaction can take place in each repeating unit of the polymer. A *macroalkoxy radical* can undergo at least three different reactions.

First, *macroalkoxy radical* ($-\text{C}(\text{O}^{\bullet})\text{H}-\text{O}-\text{C}(\text{O})-$) can convert into an anhydride (Scheme 5) ($-\text{C}(\text{O})-\text{O}-\text{C}(\text{O})-$) through a cage reaction (Structures 5a, 11, 13, 14a, 15b and 15c). Later such macromolecular anhydrides can undergo a Norrish I photocleavage reaction similar to those described above for the original polyester structure [8].

If the above described cage reaction would take place at the end group of a hydroxyl functional polymer chain (Scheme 6) (methylene group next to the alcohol group $-\text{CH}_2-\text{OH}$) a pivalic acid end group would be formed (Structures 5a, 13 and 14a). Both reactions (anhydride and pivalic acid formation) result in the same change in mass (+14 Da) with respect to structure 1a. Taking the average molecular weight of the polyester (6600 g/mol, by titration) and the mass of a repeating cluster (234 g/mol) into account the average ratio of the repeating units to the end groups is approximately 14 to 1. In this respect the probability of formation of anhydride is much



Scheme 6. Oxidation of the polymer end group.

higher than that of a pivalic acid through a cage reaction mentioned before.

An independent proof of the presence of macromolecular anhydride groups (Scheme 5) is the formation of this moiety in the molecules terminated at both ends with phthalic acid, where no confusion with pivalic acid is possible. This was indeed found as Structure 11.

The *macroalkoxy radical* ($-C(O^{\cdot})H-O-C(O)-$) can also undergo a β -scission reaction (Scheme 5). As a consequence a *carboxyl radical* B-2 and a pivalic aldehyde are formed (Structures 1b, 7b and 15c). Since some traces of a pivalic aldehyde were already detected before UV irradiation it is difficult to evaluate if this reaction really takes place. It is known that aldehyde in this conditions can easily undergo oxidation to acid (Scheme 5), (Structures 5a, 13 and 14a).

Finally, a *macroalkoxy radical* can abstract hydrogen and form a hemiacetal (Scheme 5) (Structure 15a).

In many of the mechanisms proposed in this paper, a macromolecular hydroperoxide as intermediate species is proposed. Although we have successfully identified most of the products, we could not find direct evidence of hydroperoxides in the MALDI spectra. This is probably due to their low UV and thermal stability. As intermediate products hydroperoxides are known to accumulate only in very low concentration.

4.5. Final remarks

Based on the data obtained, it is confirmed that the Norrish type I photocleavage of the ester group takes place first. In the initial stage, radicals which are formed in this reaction (directly, or after rearrangement) abstract hydrogen and form new end groups. For instance, isobutyl and isobutene end groups (Structures 3a and 3b) were identified after 1 h of irradiation. UV exposure of PNI for 1 h under nitrogen resulted in the formation of the same clustered isotopic distribution 3 attributed to isobutyl and isobutene end groups as found when UV exposed under air. This additionally confirms our interpretation of the data and proves that in the initial stage of degradation direct photocleavage followed by a hydrogen abstraction takes place. The products of oxidation are especially observed in the later stages.

The primary radicals and later formed oxy- and peroxy-radicals can abstract hydrogen. The most labile hydrogen atoms on the polyester backbone are present in the α -position of the ester group. Oxidation processes taking place in the polymer backbone can directly (β -scission) or indirectly (anhydride) lead to further fragmentation of polymer chain.

As shown above there are two mechanisms leading to fragmentation of the polymer chain, the direct Norrish type I photocleavage of aromatic esters followed by the oxidation of polymer backbone at the carbon atom involved in the cleavage.

Norrish type I photocleavage can take place at three different positions of an aromatic ester group. Based on the bond dissociation energies of a model compound (ethyl benzoate), Day and Wiles suggested that the photocleavages A (88 kcal/mol) and B (84 kcal/mol) are more favorable than photocleavage C (102 kcal/mol) [6] (Scheme 1). The experimental data obtained in this work can confirm that the degradation products, identified in this study, are all contributable to photocleavages A and B.

5. Conclusions

In this work, the molecular mechanism of the photolysis and photooxidation of a non-crosslinked poly(neopentyl isophthalate) (PNI), applied as a thin coating on an aluminium plate and irradiated with a mercury lamp, was studied.

Information on the changes in the size of the molecules was obtained by SEC. Both an increase and a decrease of molar weight were observed, indicating that crosslinking and chain scission take place simultaneously during photodegradation. Extensive exposure led to insoluble material (gel) up to 23%.

ATR-FTIR was used to detect groups such as C=O and OH/OOH generated in the polymer structure due to the break down of polymer chain by photooxidation. The changes in the range of 1800–1600 cm^{-1} could be attributed to anhydride, acids and aldehydes. Moreover, the formation of a very broad band in the range of 3600–2500 cm^{-1} indicates the presence of different types of OH groups (alcohol and carboxyl).

MALDI-ToF MS revealed the molecular structure of the degradation products from the very first reactions taking place. It has been demonstrated that Norrish type I photocleavage reactions take place, in accordance with the earlier published bond dissociation energies of the possible pathways. Radicals formed from those photocleavages can abstract hydrogens and form mainly isobutyl and phthalic acid end groups, which are observed in MALDI in the early stages of degradation. Reactions of the above mentioned radicals with oxygen lead to acid and alcohol groups, and these photooxidation products are observed in MALDI in later stages of photodegradation.

Hydrogen abstraction from the polymer backbone plays an important role in photodegradation too. Radicals formed in the α -position to the ester due to hydrogen abstraction may react with oxygen. The alkoxy radical formed as a consequence of this process can rearrange to anhydride (via a cage reaction), which possibly later breaks down e.g. by hydrolysis. The alkoxy radical may also directly decompose via β -scission. These reactions taking place along the polymer backbone account for oxidation induced decomposition of polymer.

In general, the data obtained with MALDI-ToF MS and supported by SEC and ATR-FTIR allowed to establish mechanisms of the photolysis and photooxidation on a molecular level leading to a considerably improved understanding of the degradation processes of aromatic polyester.

Acknowledgments

This research forms part of the research program of the Dutch Polymer Institute (DPI), project #419.

References

- [1] Rabek JF. Polymer photodegradation - mechanisms and experimental methods. 1st ed. London: Chapman and Hall; 1995.
- [2] White JR, Turnbull A. J Mater Sci 1994;29:584–613.
- [3] Marcotte FB, Campbell D, Cleaveland JA, Turner DT. J Polym Sci 1967;5:481–501.
- [4] Day M, Wiles DM. J Appl Polym Sci 1972;16:175–89.
- [5] Day M, Wiles DM. J Appl Polym Sci 1972;16:191–202.
- [6] Day M, Wiles DM. J Appl Polym Sci 1972;16:203–15.
- [7] Rivaton A. Polym Degrad Stab 1993;41:283–96.
- [8] Rivaton A. Polym Degrad Stab 1993;41:297–310.
- [9] Grossetete T, Rivaton A, Gardette JL, Hoyle CE, Ziemer M, Fagerburg DR, et al. Polymer 2000;41:3541–54.
- [10] Tabankia MH, Gardette JL. Polym Degrad Stab 1986;14:351–65.
- [11] Maetens D. Prog Org Coat 2007;58:172–9.
- [12] Skaja AD, Croll SG. Polym Degrad Stab 2003;79:123–31.
- [13] Carroccio S, Rizzarelli P, Puglisi C, Montaudo G. Macromolecules 2004;37:6576–86.
- [14] Carroccio S, Puglisi C, Montaudo G. Macromolecules 2004;37:6037–49.
- [15] Carroccio S, Puglisi C, Montaudo G. Macromolecules 2005;38:6863–70.
- [16] Carroccio S, Rizzarelli P, Scaltro G, Puglisi C. Polymer 2008;49:3371–81.
- [17] Staal BBP. Ph.D. Thesis. University of Technology Eindhoven; 2005. ISBN 90-386-2816-1. <http://alexandria.tue.nl/extra2/200510293.pdf>.
- [18] Lin-Vien D, Colthup NB, Fateley WG, Grasselli JG. The handbook of infrared and Raman characteristics frequencies of organic molecules. Academic Press; 1990.
- [19] Huijser S, Staal BBP, Huang J, Duchateau R, Koning CE. Angew Chem 2006;118:4210–4.